CFD ANALYSIS OF GAS - PARTICLE INTERACTION IN A CIRCULATING FLUIDIZED BED RISER

P.Ragothaman,ragoth_ceg@hotmail.com
Dr.N.V.Mahalakshmi,nvmal2001@yahoo.co.in
Institute for Energy Studies, Anna University, Chennai-25,Tamilnadu, India.
P.sudhakar,sudhaakar_68@yahoo.co.in

Abstract

Circulating fluidized bed reactors are widely applied in industry for power generation in boilers and gasifier. Computational Fluid dynamics modeling of hydrodynamics and heat transfer can be an effective tool for optimizing the flow, improve the design of such systems significantly and can supplement the need for experimental analysis. Modeling and simulation of gas-solids two-phase flow is performed aiming to study the effects on flow hydrodynamics and heat transfer in the riser column of circulating fluidized bed. The modeling and simulations of circulating fluidized bed has been done by GAMBIT 2.0.4 and FLUENT 6.2 solver respectively. An Eulerian approach is considered for fluid and particulate phases. The gas phase and particulate phase turbulences are modeled using Kinetic Theory of Granular flow and K-Epsilon models respectively. User Defined codes are developed for solid phase velocity, volume fraction, Pressure drop, viscosity, drag coefficient and heat transfer co-efficient to analyze the above parameters inside the riser Column. Results are validated with experimental data published in the literature. There is a good agreement between measured and simulated profiles of solids axial velocity and solids volume fraction along the diameter of riser at 4.9m and pressure profile along riser column of 15.08 m.

Keywords: Gas-solids flow, hydrodynamics, turbulence, eulerian, kinetic theory.

1. INTRODUCTION

Gas-solids fluidization is widely applied in industry, including petroleum, chemical, metallurgical and energy industries. The largest applications of fluidized bed reactors occur in coal combustion for large scale thermoelectric power generation, and catalytic cracking of petroleum to produce gasoline and other fuels. CFB combustors, due to the high velocity of heat and mass transfer, allow the combustion to take place at temperatures of between 1023 K and 1173 K, avoiding peaks, which are present in traditional systems, where the temperature can reach 1773 K. The absence of these peaks causes, as a direct consequence, a significant reduction of NOx and SOx emissions, as it is possible to put adsorbents directly inside the reactor.

A layer of particles is said to be fluidized when the drag exerted on the particles by an up flowing gas balances the weight of the particles when correcting for buoyancy. The superficial gas velocity at which this occurs is called the minimum fluidization velocity or the incipient fluidization velocity. When the particles are fluidized the mixture of particles and gas in many ways behave like a fluid, hence the term fluidization.

The particles are classified into four groups according to their fluidization characteristics. Group A consists of aeratable particles with a small mean diameter and/or a low density. This type of particles can be fluidized homogeneously at low gas velocities and form small bubbles at higher velocities. Group B is a group of sand-like particles that fluidize easily, but will have bubble formation at the minimum fluidization velocity. Group D are spoutable particles all the way from coarse sand up to boulders and rocks. Group C are cohesive particles that are very hard to fluidize. Flour and starch are typical examples

of this group. The particles studied in this thesis belong to group B.There are various fluidization regimes for these particles depending on the superficial gas velocity.

Hydrodynamic studies can significantly contribute for better understanding and thereby solving the problems encountered in Circulating fluidized bed (CFB). The structure of multiphase flows in circulating fluidized bed columns is very complex, showing great variations on solids volumetric fraction through the riser, continuous formation and dissipation of clusters, and a high rate of recirculation of solids. Such flow condition causes an intense superficial contact between gas and solids providing high reaction rates. The knowledge of the flow hydrodynamics is of great importance, allowing relevant reactive and mass transport parameters to be determined.

The mathematical modelling of gas-solids fluidization processes represents an ancillary tool for minimizing the experimental efforts required for developing industrial plants. Besides, mathematical models require experiment in order to be validated and, concerning fluidization, the required experiments involve complex measurements of difficult accomplishment. Therefore, mathematical modelling also represents an incentive for the development of new experimental methods and techniques.

The gas/particle flow inside a CFB unit is very complex (Fig1.1). The distribution of the particles in the riser gives a core-annulus flow with particles flowing down along the walls and strands or clusters of particles moving along with dispersed particles in the centre of the riser. The particle distribution in the riser has influence on the chemical reactions taking place and/or heat transfer properties.

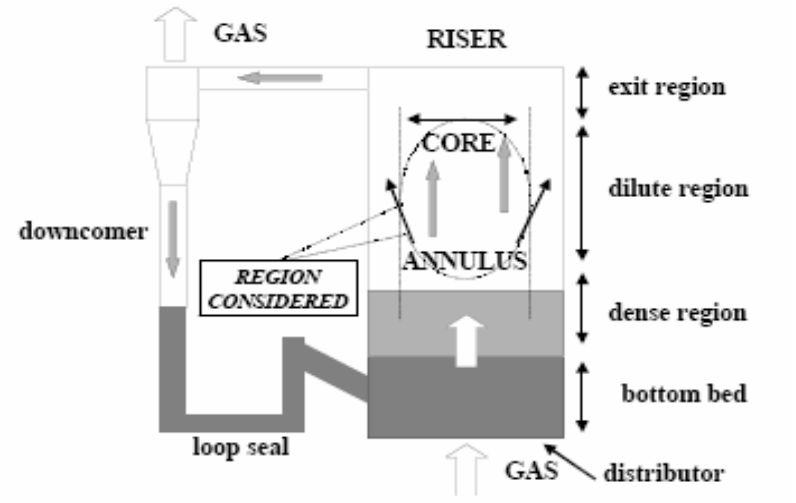

Figure 1. Multiphase flow structure of CFBC

Design of CFB units affects the flow patterns inside the unit and hence the performance of the unit. The design process is mainly been based on experience from other units, experiments with scaled models and empirical models. But this process is very expensive and the units do not show as good performances as the scaled units due to lack of good design tools for scale-up.

The focus of this work will be on three-dimensional multiphase numerical studies of gas/particle flow in CFB riser unit considering the influence of turbulence behaviour of both gas and solid phases.Based on the results recommendations will be given for modeling of riser flows. All the studies performed will be evaluated against experimental data from the literature.

2 .NUMERICAL MODELS

The industrial scale simulations uses the multifluid Eulerian/Eulerian approach is normally used as the number of particles in the CFB reactors are well above 10^{12} . The model used in this work is based on the multifluid Eulerian-Eulerian approach. Each phase, identified through its volume fraction, is treated as a continuum medium, which interpenetrates into other phases. Both a continuity (1) and a momentum equation (2) were solved independently for each phase, obtaining the coupling of phases through a drag term. A two-fluid model, are more suitable for research allowing, for instance, the behaviour of local flow structures and the effects of local geometry. The turbulence governing equations for both solid and gas phases are derived from the KTGF approach. The KTGF is based on an analogy between the flow of granular materials and the motion of gas molecules.

2.1 EULERIAN MODEL

The volume fraction of each phase is calculated from a continuity equation

$$\frac{\partial}{\partial t}(\alpha_i \rho_i) + \nabla \cdot (\alpha_i \rho_i \vec{v}_i) = 0 \tag{1}$$

The fluid-solid momentum equation,

$$\frac{\partial}{\partial t}(\alpha_i \rho_i \vec{v}_i) + \nabla \cdot (\alpha_i \rho_i \vec{v}_i \vec{v}_i) = -\alpha_i \nabla P + \nabla \cdot \bar{\bar{\tau}} - \beta(\vec{v}_i - \vec{v}_j) + \rho_i \alpha_i \vec{g} \tag{2}$$

2.2 DRAG FACTOR

For getting best results, we have used the improved drag correlation rather than that of Syamlal-O'Brien's default drag factor.The improved drag correlation given by Hill Koch lad model is

$$\beta_{gm} = \frac{3}{4} C_D \frac{\rho_g \varepsilon_g \varepsilon_m \left| u_g - u_m \right|}{d_{vm}} \varepsilon_g^{-2.65} \tag{3}$$

The drag force (F) is given as:

$$F = 1 + 3/8\,\mathrm{Re} \qquad \varepsilon_s \le 0.01 \; and \; \mathrm{Re} \le \frac{(F_2 - 1)}{(3/8 - F_3)}$$

$$F = F_0 + F_1 R_e^2 \qquad \varepsilon_s > 0.01 \; and \; \mathrm{Re} \le \frac{F_3 + \sqrt{F_3^2 - 4F_1(F_0 - F_2)}}{2F_1}$$

$$F = F_2 + F_3\,\mathrm{Re} \qquad \begin{cases} \varepsilon_s \le 0.01 \; and \; \mathrm{Re} > \dfrac{(F_2 - 1)}{(3/8 - F_3)} \\ \varepsilon_s > 0.01 \; and \; \mathrm{Re} > \dfrac{F_3 + \sqrt{F_3^2 - 4F_1(F_0 - F_2)}}{2F_1} \end{cases}$$

$$F_0 = \begin{cases} (1-w)\left[\dfrac{1+3\sqrt{\varepsilon_s/2}+(135/64)\varepsilon_s\ln(\varepsilon_s)+17.14\varepsilon_s}{1+0.681\varepsilon_s-8.48\varepsilon_s^{\,2}+8.16\varepsilon_s^{\,3}}\right]+w\left[10\dfrac{\varepsilon_s}{(1-\varepsilon_s)^3}\right] & 0.01<\varepsilon_s<0.4 \\ 10\dfrac{\varepsilon_s}{(1-\varepsilon_s)^3} & \varepsilon_s \geq 0.4 \end{cases}$$

$$F_1 = \begin{cases} \sqrt{\dfrac{2}{\varepsilon_s}}/40 & 0.01<\varepsilon_s \leq 0.1 \\ 0.11+0.00051\exp(11.6\varepsilon_s) & \varepsilon_s > 0.1 \end{cases}$$

$$F_2 = \begin{cases} (1-w)\left[\dfrac{1+3\sqrt{\varepsilon_s/2}+(135/64)\varepsilon_s\ln(\varepsilon_s)+17.89\varepsilon_s}{1+0.681\varepsilon_s-11.03\varepsilon_s^{\,2}+15.41\varepsilon_s^{\,3}}\right]+w\left[10\dfrac{\varepsilon_s}{(1-\varepsilon_s)^3}\right] & \varepsilon_s<0.4 \\ 10\dfrac{\varepsilon_s}{(1-\varepsilon_s)^3} & \varepsilon_s \geq 0.4 \end{cases}$$

$$F_3 = \begin{cases} 0.935\varepsilon_s+0.03667 & \varepsilon_s<0.0953 \\ 0.0673+0.212\varepsilon_s+0.0232/(1-\varepsilon_s)^5 & \varepsilon_s \geq 0.0953 \end{cases}$$

$$\mathrm{Re} = \frac{\rho_g(1-\varepsilon_m)\left|u_g-u_m\right|d_{pm}}{2\mu_g}$$

$$w = e^{(-10(0.4-\varepsilon_s)/\varepsilon_s)}$$

SOLID-SOLID EXCHANGE COEFFICIENT

$$K_{ls} = \frac{3(1+e_{ls})\left(\frac{\pi}{2}+C_{\mathrm{fr},ls}\frac{\pi^2}{8}\right)\alpha_s\rho_s\alpha_l\rho_l(d_l+d_s)^2 g_{0,ls}}{2\pi(\rho_l d_l^3+\rho_s d_s^3)}|\vec{v}_l-\vec{v}_s| \qquad (4)$$

2.3 GRANULAR TEMPERATURE

The solid phase properties were calculated using the kinetic theory for granular flows, which allows the solid viscosity to be determined as a function of the granular temperature Θs, which had been determined using both the simplified algebraic equation implemented by FLUENT. The closure equations of the kinetic theory are summed up in Table 1.

$$\left(-P_s\bar{\bar{I}}+\bar{\bar{\tau}}_s\right):\nabla\vec{v}_s-\gamma_s+\Phi_s=0$$

$$\frac{3}{2}\left[\frac{\partial}{\partial t}(\alpha_s\rho_s\Theta_s)+\nabla\cdot(\alpha_s\rho_s\Theta_s)\right]=\left(-P_s\bar{\bar{I}}+\bar{\bar{\tau}}_s\right):\nabla\vec{v}_s+$$

$$+\nabla\cdot(k_s\nabla\Theta_s)-\gamma_s-3\beta\Theta_s \qquad \textbf{(5)}$$

Table 1: Kinetic theory closure equations

Granular pressure

$$P_s = \alpha_s \rho_s \Theta_s + 2\rho_s (1+e)\, \alpha_s^2 g_0 \Theta_s$$

Radial distribution function

$$g_0 = \left[1 - \left(\frac{\alpha_s}{\alpha_{s,\max}}\right)\right]^{-1}$$

Solid phase kinetic viscosity – Syamlal [32]

$$\mu_{s,kin} = \frac{\alpha_s d_p \rho_s \sqrt{\pi \Theta_s}}{6(3-e)}\left[1 + \frac{2}{5}\alpha_s g_0 (1+e)(3e-1)\right]$$

Solid phase kinetic viscosity – Gidaspow [11]

$$\mu_{s,kin} = \frac{10 d_p \rho_s \sqrt{\pi \Theta_s}}{96 \alpha_s g_0 (1+e)}\left[1 + \frac{4}{5}\alpha_s g_0\right]$$

Solid bulk viscosity [19]

$$\lambda_s = \frac{4}{3}\alpha_s \rho_s d_p g_0 (1+e)\left(\frac{\Theta_s}{\pi}\right)^{\frac{1}{2}}$$

Solid frictional viscosity

$$\mu_{s,fr} = \frac{P_s \sin\varphi}{2\sqrt{I_{2D}}}$$

Solid phase laminar viscosity

$$\mu_s = \mu_{s,col} + \mu_{s,kin} + \mu_{s,fr}$$

Collisional dissipation term of the granular phase

$$\gamma_s = 3\alpha_s \rho_s g_0 \Theta_s (1-e^2)\left[\frac{4}{d_p}\left(\frac{\Theta_s}{\pi}\right) - \nabla \cdot \vec{v}_s\right]$$

Solid phase conductivity - Syamlal

$$\kappa_s = \frac{15 d_p \rho_s \alpha_s \sqrt{\pi \Theta_s}}{4(41-33\eta)}\left[1 + \frac{12}{5}\eta^2 (4\eta - 3)\alpha_s g_0 + \frac{16}{15\pi}(41-33\eta)\eta \alpha_s g_0\right]$$

Solid phase conductivity - Gidaspow

$$\kappa_s = \frac{150 d_p \rho_s \sqrt{\pi \Theta_s}}{384 g_0 (1+e)}\left[1 + \frac{6}{5} g_0 \alpha_s (1+e)\right]^2 + 2\alpha_s^2 \rho_s d_p g_0 (1+e)\left(\frac{\Theta_s}{\pi}\right)^{\frac{1}{2}}$$

$$\eta = \frac{1}{2}(1+e)$$

3. K- Є TURBULENCE MODEL FOR EACH PHASE

Turbulence consists of fluctuations in the flow field in time and space.By solving two additional transport equations for each secondary phase, the per-phase turbulence model is more computationally intensive.

$$\frac{\partial}{\partial t}(\alpha_i \rho_i k_i) + \nabla \cdot (\alpha_i \rho_i \vec{U}_i k_i) = \nabla \cdot \left(\alpha_i \frac{\mu_{t,i}}{\sigma_k} \nabla k_i\right) + (\alpha_i G_{k,i} - \alpha_i \rho_i \varepsilon_i) + \beta(C_{ji} k_j - C_{ij} k_i)$$

$$\frac{\partial}{\partial t}(\alpha_i \rho_i \varepsilon_i) + \nabla \cdot (\alpha_i \rho_i \vec{U}_i \varepsilon_i) = \nabla \cdot \left(\alpha_i \frac{\mu_{t,i}}{\sigma_k} \nabla \varepsilon_i\right) + \frac{\varepsilon_i}{k_i}\left[C_{1,\varepsilon} \alpha_i G_{k,i} - C_{2\varepsilon} \alpha_i \rho_i \varepsilon_i + C_{3\varepsilon} \beta(C_{ji} k_j - C_{ij} k_i)\right] \quad (6)$$

The constants of the model were set as follows: $C1\varepsilon = 1.44$, $C2\varepsilon = 1.92$, $C\mu = 0.09$, $\sigma\kappa = 1.0$, $\sigma\varepsilon = 1.3$, $Ci,j = 2$, $Cj,i = 2\eta j,i/(1+\eta j,i)$, with $\eta j,i = \tau t,ij/\tau F,ij$.

4. ENERGY EQUATION CONSTITUTIVE MODELS

To describe the conservation of energy in Eulerian multiphase applications, a separate enthalpy equation can be written for each phase

$$\frac{\partial}{\partial t}(\alpha_q \rho_q h_q) + \nabla \cdot (\alpha_q \rho_q \vec{u}_q h_q) = -\alpha_q \frac{\partial p_q}{\partial t} + \bar{\bar{\tau}}_q : \nabla \vec{u}_q - \nabla \cdot \vec{q}_q + S_q + \sum_{p=1}^{n}(\vec{Q}_{pq} + \dot{m}_{pq} h_{pq} - \dot{m}_{qp} h_{qp}) \quad (7)$$

$$C_{1\epsilon} = 1.44, \quad C_2 = 1.9, \quad \sigma_k = 1.0, \quad \sigma_\epsilon = 1.2$$

4.1 INTERPHASE HEAT TRANSFER

$$\gamma_{gm} = C_{pg} R_{gm} \Big/ \left[\exp\left(\frac{C_{pg} R_{gm}}{\gamma_{gm}^{0}} \right) - 1 \right]$$

$$\gamma_{gm}^{0} = 6\kappa_g \varepsilon_m Nu_m \Big/ d_m^2$$

$$Nu_m = \left(7 - 10\varepsilon_g + 5\varepsilon_g^2\right)\left(1 + 0.7\,\mathrm{Re}_m^{0.2}\,\mathrm{Pr}^{1/3}\right) + \left(1.33 - 2.4\varepsilon_g + 1.2\,\varepsilon_g^2\right)\mathrm{Re}_m^{0.7}\,\mathrm{Pr}^{1/3} \quad (8)$$

5. NUMERICAL SIMULATION

5.1 BOUNDARY CONDITIONS

Parabolic profiles were adopted at the inlets of the riser for the velocity of solids(unsteady) and air(steady) ,pressure, volume fraction .Blasius and von-korman profiles were adopted for turbulent kinetic energy , turbulent dissipation rate and turbulent viscosity.. A continuity outflow condition was adopted for the outlet. A no-slip boundary condition was applied to the wall for both phases, while Neumann conditions were imposed for the granular temperature and turbulent kinetic energy. All the calculations were carried out starting from an empty riser, with a zero initial velocity for all the phases.

Parabolic Inlet velocity profile:

Fluid phase (steady): $Uy = 4.979\text{-}4.979*(x/0.0381)^2$ (9)

Solid phase (Unsteady): $v_y = 0.386+0.1*COS(10*t)$ (10)

Steady parabolic outlet pressure profile : P=121.59*105-104(y/0.0381)2 (11)

Particle volume fraction: Initial VOF = 0.6 Final VOF = 0.0246 (12)

5.2 SOLVER SETTINGS

All the equations of the model reported were solved with the finite-volume multi grid numerical approach that is available in FLUENT. Phase coupling was achieved through the PC-SIMPLE algorithm, while the convective terms of all the conservation equations were discretized with a second order upwind method. Under-relaxation factors were set as shown in Table 3. All the calculations were performed in unsteady conditions, due to the strictly unsteady behaviour of the gas-solid flow in the risers. A first-order implicit method with adaptive time stepping was adopted. Under relaxation factor for pressure is modified to 0.6 from o.3.

Table 1: Numerical flow parameters

Solid phase density,	2660 kg/m3
Solid mean diameter	140 μm
Particle mass Flux	17 kg/m2s
Air mass flow	0.6032 kg/s
Laminar gas viscosity, $\mu_{lam,g}$	1.8*10−5 kg/ms
Turbulent viscosity, μ_t	0.509kg/ms
Maximum solid packing	0.60-0.0246
rid resolution (Number of cells)	140568

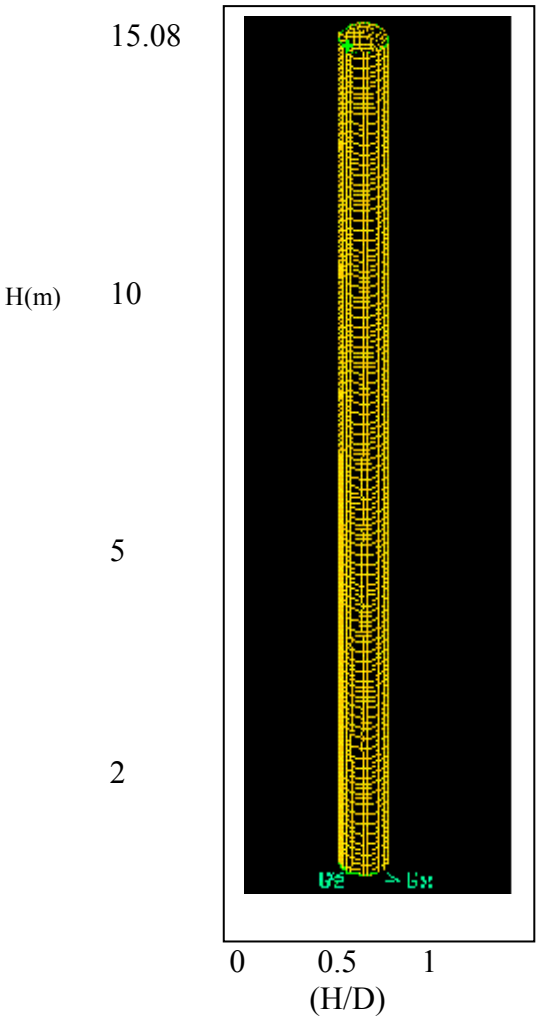

Figure 2 3D computational grid-CFB Riser from experimental setup of Werther and Hartge (2002)

5. RESULTS OF 3D-DIMENSIONAL SIMULATIONS

The experimental findings of solids axial velocity,volume fraction and pressure gradient in the riser at three different elevations corresponding to 4.9m,6.43m and 8.43m in the riser are compared with simulated profiles and validated.

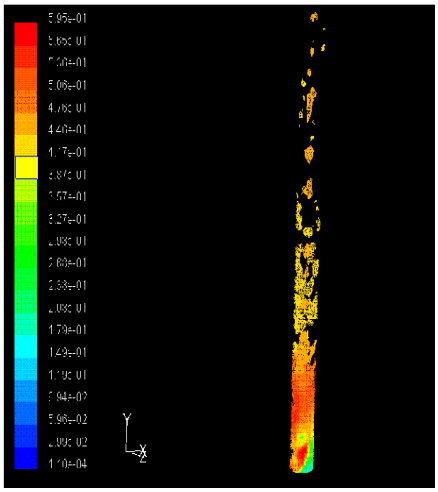

5.1 Contours of solid volume fraction along riser

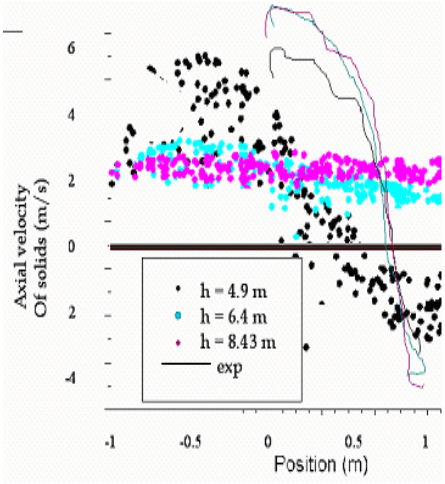

5.2 Variation of axial velocity across riser

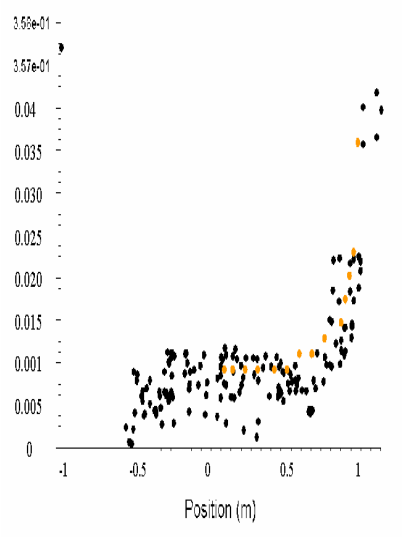

5.3 Variation of solids volume fraction across riser

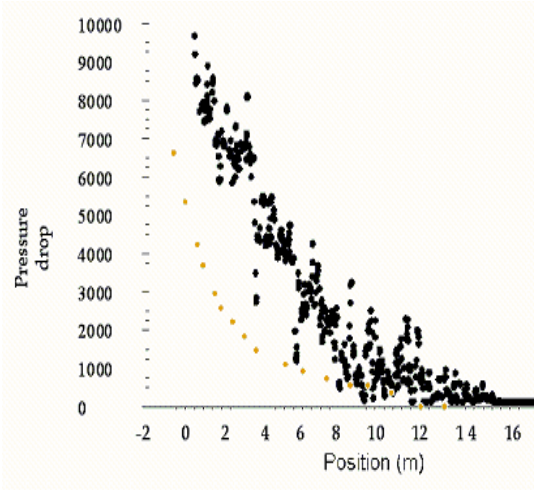

5.4 Variation of pressure drop long riser

6. CONCLUSIONS:

- The experiments profiles resemble a plug-flow with a parabolic shape with having high positive velocity in the center of the riser and negative velocity near the wall
- Smoother radial solids velocity profiles in combination with lower mass flux rates indicate narrow resistance time distributions of solids in the reactor.
- There is a good agreement between the measured and simulated profiles of solids axial velocity and volume fraction along the diameter of riser at 4.9 m.
- The solid volume fraction profile is almost straight so the gradient in solids volume fraction is very small at 6.4 m and 8.43 m.
- Due to the good back mixing predicted in the simulation, the large pressure gradient in the lower part of the riser is captured.
- The local flow pattern change dramatically with increasing static pressure. Higher static pressure improves the axial solids distribution and leads to a more homogeneous radial distribution as well.
- The Hill koch drag correlation, together with the correlation for the kinetic contribution to the turbulent viscosity of the granular phase, seems to give better results.

7. NOMENCLATURE

Symbol	Description	Unit
C_D	Drag coefficient	
C_g	Instantaneous velocity vector of the gas phase	m s^{-1}
C_s	Instantaneous velocity vector of the solid phase	m s^{-1}
D	Diameter of the riser	m
d_p	Particle diameter	µm
e	Restitution coefficient	dimensionless
g_0	Radial distribution function	dimensionless
G_s	Solid mass flux	kg s^{-1} m^{-2}
H	Height of the riser	m
Re	Reynolds number	dimensionless
k	Turbulent kinetic energy	m^2 s^2
P	Pressure	Pa
P_s	Granular pressure	Pa

U_g	Superficial gas velocity	m s^{-1}
v_i, v_j	Velocity of the phase *i* [m s^{-1}]	m s^{-1}
$v_{r,s}$	Terminal velocity of the particles	m s^{-1}

Greek letters

α	Volume fraction	dimensionless
γ_s	Collisional dissipation of the granular energy	
μ	Viscosity	Pa s
ε	Turbulent dissipation rate	m^2 s^{-3}
ρ	Density	kg m^{-3}
Θ_s	Solid granular temperature	m^2 s^2
κ_s	Solid phase conductivity	
$\tau_{L,ij}$	Lagrangian integral time scale	s
$\tau_{F,ij}$	Particle relaxation time	s
φ	Angle of friction	rad

Subscript

g	Gas phase
s	Solid phase

8.References

1. C.H.Ibsen et al, " Evaluation of 3D numerical model of scaled circulating fluidized bed".ACS,2001,Denmark.

2. L.C.Gomez et al," Gas – solid two phase flow in riser of circulating fluidized beds",JBSMS,2001,Brazil.

3. K.G.Hansen et al," An experimental and computational study of gas particle flow in scaled circulating fluidized bed",WCPT,2002,Australia.

4. K.G.Hansen," A 3D numerical study of gas particle flow and chemical reactions in circulating bed reactors",Ph.D thesis,GCFFP,2005,Denmark

5. Paul cizmas, " A reduced order model of two-pahase flow,heat transfer and combustion in circulating fluidized beds",TEES,2003,USA.

6. Balzer,G.,Simonin,O.,Boelle,A. and Lavieville,J.,1996,"Circulating fluid bed technology,Science press,Beijing,p.432-439.

7. Boemer,A.,Qi,H.,Renz,U.,Vasquez,s and Boysan,F.,1995,"Eulerian computation of fluidized hydrodynamics",Proc 13th Int. Conf. on Fluidized Bed Combustion,V2,p 775-787